Received: 8 May 2015 ■ Revised: 5 January 2016 ■ Accepted: 6 January 2016 ■ Publication: 19 January 2016

JNIRS JOURNAL OF NEAR INFRARED SPECTROSCOPY

Development of a handheld spectrometer based on a linear variable filter and a complementary metal-oxide-semiconductor detector for measuring the internal quality of fruit

Xinyang Yu,[a,b] Qipeng Lu,[a]* Hongzhi Gao[a] and Haiquan Ding[a]

[a]State Key Laboratory of Applied Optics, Changchun Institute of Optics, Fine Mechanics and Physics, Chinese Academy of Sciences, Changchun 130033, PR China. E-mail: luqipeng@126.com

[b]Graduate University of Chinese Academy of Sciences, Beijing 100049, PR China

Visible and near infrared spectroscopy has long been used to predict fruit internal quality, with portable instrumentation advantageous for in-field use. We developed a handheld spectrometer using a linear variable filter (LVF) and a complementary metal-oxide-semiconductor (CMOS) linear detector array. The LVF is a bandpass filter with a centre wavelength changing linearly in one direction and can replace a grating as the light-dispersion component. An LVF was designed and fabricated specifically to work in the 620–1080 nm region and for the analysis of fruit. The optical design used an improved collimator and an LVF to yield a compact, stable and low-cost optical engine. By using a CMOS detector and other suitable electronics, the spectrometer achieved a low power consumption. The spectrometer can analyse spectral data using an onboard prediction model and can be operated from a remote smartphone, tablet or laptop computer. This paper details the design of the spectrometer and the results of its resolution and stability tests. The spectrometer operated with a resolution of less than 1.5% centre wavelength and a signal-to-noise ratio of up to 5000. The spectrometer was then used to predict the sugar content in pears. The optimised model provided an R^2c value of 0.96, standard error of calibration value of 0.29 °Bx and standard error of prediction value of 0.46 °Bx. The results indicated that this LVF-based spectrometer is promising for measuring the internal quality of fruit.

Keywords: Brix, fruit, linear variable filter, visible, near infrared, handheld, interactance, CMOS detector, signal-to-noise ratio, PLS, sugar content

Introduction

Near infrared (NIR) spectral analysis offers the advantages of being noninvasive and efficient. It has long been used to evaluate internal quality of fruit.[1] Most commercial spectrometers focusing on this application use visible and shortwave near infrared spectra, and most application research is carried out in this optical region, because: (1) the bands are ascribed to the third and fourth overtones of O–H and C–H stretching modes;[2] (2) silicon linear detector arrays are much cheaper than InGaAs arrays; and (3) the penetration depth is deeper for short-wavelength NIR radiation than by longer-wavelength NIR radiation.[3]

Fruit may be assessed using vis-NIR spectroscopy in the orchard, in the storehouse, on the grading line or in the market. Therefore, most applications are on-site measurements, which

ISSN: 0967-0335
doi: 10.1255/jnirs.1191

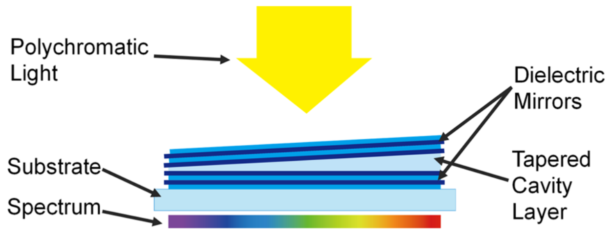

Figure 1. Working principle of a type of linear variable filter. Two mirrors consisting of dielectric layers are on either side of the cavity.

require portable tools. Currently, several portable instruments focused on fruit detecting are commercially available, such as "Fruit Tester 20" and "NIR-Gun" (FANTEC, Kosai-city, Japan), "QS_300" (Unitec S.p.A., Ravenna, Italy), "F750" (Felix Instruments, Camas, WA) and "AccuNIR2200" (Ocean Optics, Dunedin, FL). Those devices are grating-based spectrometers. Over the last decades, microelectromechanical systems (MEMS) technology has been utilised in various new miniature spectrometers. Those instruments are compact but contain high-cost optical components, which makes them too expensive for widespread adoption by the fruit industry.

The linear variable filter (LVF) features a transmission function varying in one direction. Fabry–Pérot-type linear variable bandpass filter is a Fabry–Pérot bandpass filter with a varying central wavelength. The central wavelength of a typical Fabry–Pérot-type bandpass filter is $\lambda = 2nt/N$, where t is the thickness of the resonator cavity layer, n is the refractive index of cavity layer, and N is the resonance order. A Fabry–Pérot-type LVF has a tapered cavity layer as shown in Figure 1. Thus, the central wavelength of the LVF is a function of the position and varies continuously along the variable direction as t changes. The LVF can disperse incident light into a spectrum at the plane of the filter.

An LVF-based spectrometer is obtained by mounting an LVF directly on a linear detector array. Compared with grating-based instrument, the advantages of the LVF-based spectrometer are a short optical train, large optical throughput and high stability, which make it highly suitable for being built into a portable device. Moreover, low-cost LVFs are available as coating technology develops. The MicroNIR^{TM} spectrometer developed by JDSU (now Viavi, Santa Rosa, CA) was obtained by mounting an LVF on an InGaAs array detector. The device weighs 60 g and is less than 50 mm in diameter. Several recently published works showed promising performance results for both qualitative and quantitative assessments.[4,5]

We developed a handheld spectrometer with an LVF to predict the internal quality of fruit. First, an LVF was designed and fabricated specially for the visible and shortwave near infrared (vis-NIR) region to be suitable for the analysis of fruit. A compact optical engine was obtained with an improved collimator and LVF. A complementary metal-oxide-semiconductor (CMOS) detector was used instead of a charge-coupled device (CCD) detector, to yield a high signal-to-noise ratio. The electronic system has a low noise and low power consumption, and is equipped with a wireless communication module. After the spectrometer was constructed, we set up an experiment to test its performance to assess the internal quality of pear.

Materials and methods

Spectrometer

The spectrometer is a gun-shaped device as shown in Figure 2. The optical engine at the front of the spectrometer is ultra-compact. The light source surrounds the entrance window. Light penetrates through part of the fruit flesh, enters the window and then is dispersed by an LVF, and the spectrum is detected by a linear detector array.

With one pull of the trigger button, the instrument collects a spectrum, processes the spectral data using the prediction model and displays results on a screen. A Li-ion battery in the handle provides the power. The spectrometer can send the spectrum of the sample to a smartphone, tablet or laptop computer wirelessly.

Linear variable filter

The LVF was designed for fruit internal quality analysis and provides vis-NIR wavelengths in the region 620–1080 nm. The LVF length is 12.8 mm, which is the active-area length of a standard 12.8 mm linear detector array. The spatial gradient of the central wavelength is 35.9 nm mm^{-1}. The transmission function of each band is a Gaussian curve. The full width at half maximum (FWHM), which indicates spectral resolution, was designed to be less than 1.5% centre wavelength, that is 9.3 nm at a wavelength of 620 nm, and 16.2 nm at 1080 nm. This resolution is suitable to detect absorption peaks in this region. A wavelength resolution below 10 nm is probably not necessary,[2,6,7] and a higher resolution would mean a trade-off in the spectral range.

The LVF was fabricated using a dual-ion-beam sputtering system (Veeco Instruments, Santa Barbara, CA). We made LVFs in large quantities, thereby making each filter as cheap as the most common grating. An image of the LVF is shown in Figure 3.

The filter was scanned through its length with a microspectrophotometer and a Fourier transform spectrometer. The spectral response of a linear variable filter was measured

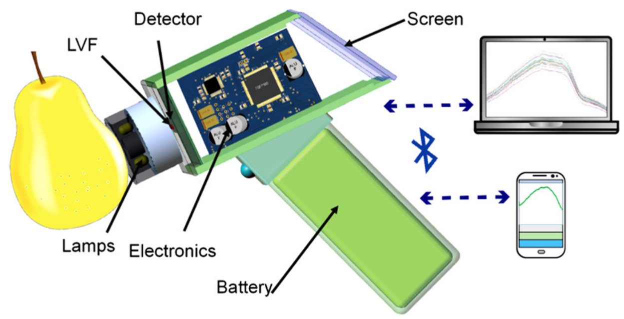

Figure 2. Schematic of the spectrometer.

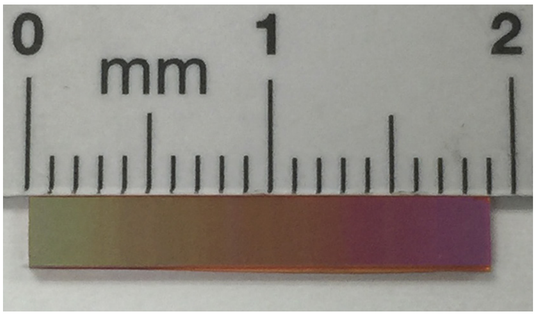

Figure 3. Linear variable filter. The length of the effective area is 12.8 mm.

with a Nicolet 6700 Fourier transform spectrometer (Thermo Fischer Scientific, Madison, WI) at a resolution of 2 cm^{-1}. The filter was placed at the sample plane during the scan. A 40 μm slit was placed tightly behind the LVF. The filter was shifted along its length with 0.5 mm steps for each measurement to complete the scan. The measured peak transmittances were in the 65–75% range (Figure 4). Each transmission peak had an FWHM of less than 1.5% centre wavelength.

Similar to the situation for a grating-based spectrometer, spectra of different orders may overlap in an LVF-based spectrometer, and so a long-pass filer was used as an order-sorting filter to block the spectrum below 540 nm. Long-pass coatings were deposited on the other side of the substrate opposite the LVF coatings.

Optical design

Three types of measurement modes are frequently used to obtain near infrared spectra of fruit: transmission, reflectance and interactance.[8] Research suggests that the transmittance mode and interactance mode provide more accurate results than the reflectance mode.[9] Compared with the transmittance mode, the interactance mode needs a lower light intensity, thus consuming less power. Our spectrometer acquires spectra by the interactance mode.

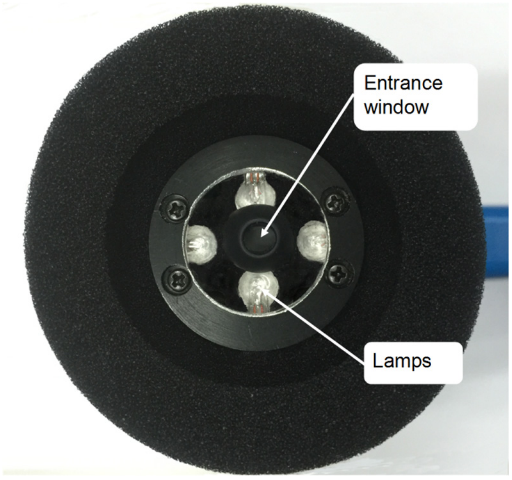

Figure 5. Front view of the measuring head of the spectrometer.

As Figures 5 and 6 show, the light source consisted of four tungsten lamps placed symmetrically around the entrance window, with the filament plane parallel to the entrance window surface. Light from the source entered the fruit and penetrated part of the tissue, and that which emerged from the fruit entered the window. A 6-mm-diameter rubber grommet surrounded the entrance window and acted as a light seal, thus preventing surface-scattered light from reaching the window directly. A very soft black foam ring around the

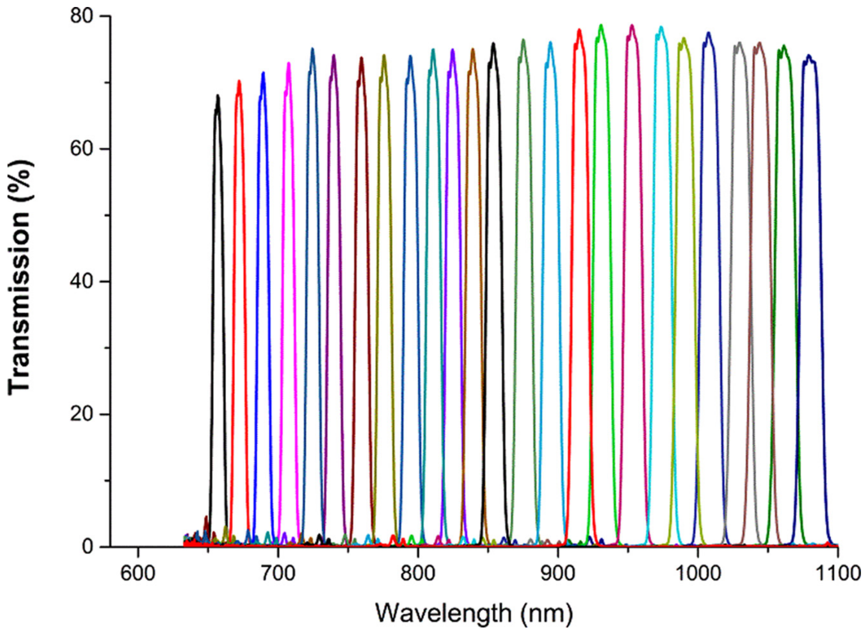

Figure 4. LVF spectral transmittances measured using the Fourier transform spectrometer.

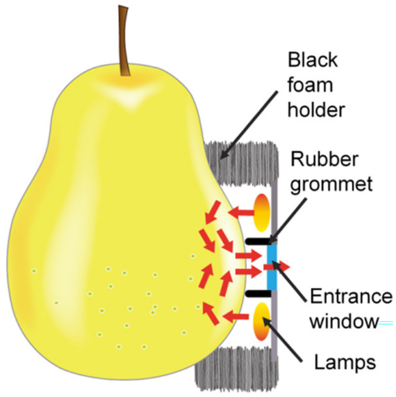

Figure 6. Schematic illustration of the measuring head of the spectrometer.

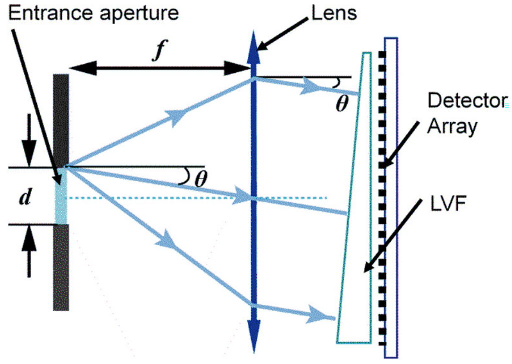

Figure 7. Layout of the optical design used in the spectrometer.

detector head supported the fruit and shielded it from external light. While a spectrum was being acquired, the fruit was held gently, but firmly, against the foam ring to ensure that the rubber grommet was also firmly against the fruit surface.

An LVF spectrometer does not need a slit, thereby being advantageous in terms of optical throughput. However, as for normal Fabry–Pérot filters, the LVF needs a collimated light source. Narrow band filters are sensitive to the incidence angle. When the incidence angle increases, the central wavelength shifts, the FWHM worsens, and some sidebands may ripple. The shift $\Delta\lambda$ of the central wavelength at an angle θ was calculated as:[10]

$$\Delta\lambda = \frac{\lambda_0\theta^2}{2{\mu_\#}^2} \tag{1}$$

λ_0 is the central wavelength and $\mu_\#$ is a type of effective refractive index for the coating. At an angle of 5°, the shift is less than 0.08% central wavelength, which is about 5% of the band width. Such deterioration is acceptable for an LVF with a spectral resolution of 1.5% centre wavelength. The changes in peak transmittance and band width were negligible.

We simulated prism light guide, fibre bundle and other designs to collimate the light and modify the light beam to the shape of the linear detector array. However, these methods either reduce resolution or complicate the optical engine. Figure 7 shows the current design, an optimised collimator. The entrance aperture was at the front focal plane of the lens. A piece of frosted glass (the entrance window) was placed at the position of the entrance aperture to diffuse the incident light evenly. Any rays that passed through the same point of the front focal plane would emerge from the lens parallel to each other and have the same incidence angle. Rays from the periphery of the window give the largest incidence angle: $\sin\theta = d/2f$, where d is the diameter of the entrance window, and f is the focal length of the lens. For our instrument, the diameter of the entrance aperture was 6 mm, and the focal length was 40 mm. Therefore, the maximum incidence angle was less than 5°. Although reduced by the collimator, the optical throughput is still sufficient to ensure a relatively short integration time. The integration time was set to 150 ms with the current light source, when we measured pear and apple samples. This kind of structure is simple, inexpensive and rugged. The LVF was mounted atop the detector chip with the long-pass filter coating facing the entrance. The gap between filter and detector was minimised to avoid any loss in resolution. The optical bench was therefore compact owing to the short optical train.

The detector resolution should suit the resolution of the LVF.[11] The LVF has a spectral resolution (FWHM) of less than 1.5% centre wavelength. At a wavelength of 620 nm, the resolution was 9.3 nm, equivalent to 259 µm in terms of distance along the LVF. The LVF bandpass shape was an approximate Gaussian curve. In this situation, the Nyquist criterion was 2.355 (FWHM = 2.355 pixels). A 128-element linear detector array with 100-µm pixel pitch was suitable, since 2.355 pixels is equivalent to 235.5 µm, which is smaller than 259 µm. However, the pixels of the detector are not ideal points. A 256-element detector with a 50-µm pixel pitch provides a higher spectral resolution, but a detector with 512 or more elements would not have improved the resolving power, since the resolution was limited by the LVF. A smaller pixel size would drop the response by the detector. Hence, a 256-element detector was applied.

Detector and electronics

To detect vis-NIR radiation, two kinds of silicon detect array are available: (1) a CCD linear detector array; (2) a CMOS linear detector array or photodiode array (PDA). The advantage of a CCD is the high sensitivity. In conventional grating spectrometers, a high sensitivity is crucial for high resolution because the slit rejects most light, and so a CCD is selected, but a CCD has a low maximum signal-to-noise ratio because it is easily saturated. By contrast, a CMOS has a larger saturation output charge, producing a much higher maximum signal-to-noise ratio. Most CMOS detector arrays have a signal-to-noise ratio of 2000–10,000, as compared with less than 1000 for most CCDs. LVF spectrometers have a larger optical throughput than grating spectrometers, and a case higher light intensity is available. In addition, NIR spectral bands overlap with each other, thereby producing no deep valleys in the 620–1080 nm

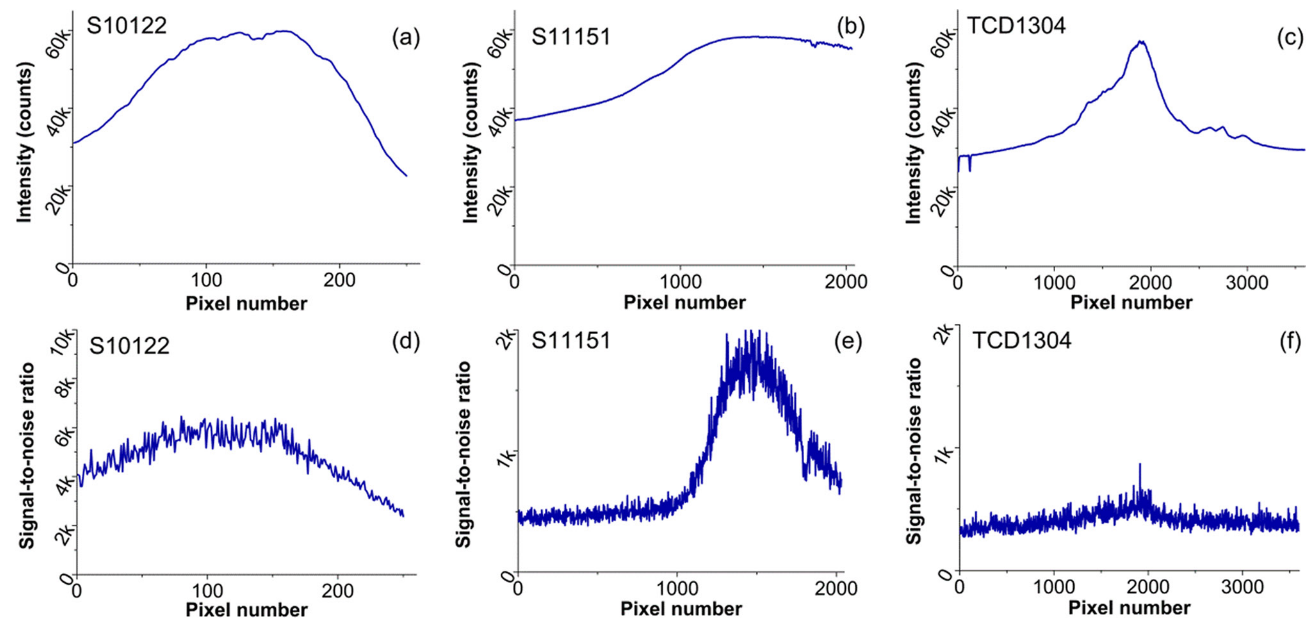

Figure 8. (a–c) Signal intensity and (d–f) signal-to-noise ratio of three linear detector arrays. (a) and (d) show the results with CMOS S10122, (b) and (e) show the results with CCD S11151, (c) and (f) show the results with CCD TCD1304.

region. Furthermore, quantitative analysis specifically requires a high signal-to-noise ratio, and so a CMOS detector was chosen (Figure 8).

The spectrometer uses a CMOS detector with a large saturation output charge, low noise and low power requirements (S10122-256Q; Hamamatsu Photonics Co., Hamamatsu, Japan). We compared this detector with two CCD detectors. One was an S11151 (Hamamatsu Photonics Co.), and the other was a TCD1304 (Toshiba, Tokyo, Japan), which is widely used in grating-based spectrometers. Each detector's response was set at near saturation level (around 60,000 counts, the range is 0–65,535) with the same integration time of 25 ms, by altering the light level. To evaluate the signal-to-noise ratio, the mean was divided by the root-mean-square noise at each wavelength. We calculated the standard deviation of 100 spectra to characterise the root-mean-square noise. The S10122 had a superior signal-to-noise ratio up to 5000 or higher, compared with a value of about 1500 for the S11151 and only 500 for TCD1304.

Moreover, the CMOS detector was easy to drive. The CMOS detector operates from a single power supply, while a CCD requires more than one power supply. Besides, a CMOS detector has a low power dissipation and is suitable for battery-powered equipment. The S10122-256Q consumed only 3.5 mW of power, compared with the 10–100 mW consumption needed by conventional CCD detectors.

With a clamping circuit, the signal-readout circuit minimises the noise and restores the direct-current level. The 16-bit analog-to-digital converter digitizes signals. Then, the CPU analyses spectral data using onboard models, and an LCD screen displays fruit quality attributes. The power supply was a quick-charge, replaceable lithium-ion polymer battery. Low-dropout (LDO) regulators and DC–DC converters are power-supply components widely used in portable devices. Although a DC–DC converter would be more efficient, the LDO regulator can provide a voltage source with a lower noise, which is highly desirable for quantitative analysis. A 7.4 V battery (two standard battery packs in series) with an LDO regulator was used instead of a 3.7 V standard battery with a DC–DC converter.

A large touch screen and powerful CPU were not used, as these would increase the power consumption and reduce battery life dramatically. Instead, the spectrometer was equipped with a low-power wireless module to communicate with, and be controlled by, computers, smartphones and tablets wirelessly. The spectrometer can obtain and deliver spectral data to a smartphone where it can be displayed along with quality attributes on the screen, or analysed further. In addition, smartphones can be programmed to build models with received data, or simply download models from the Internet and then update the spectrometer. This combination is suitable for on-site applications. We have already developed programs for computers and smartphones to operate the instrument.

Samples and spectra acquisition

To determine the potential performance in internal quality predicting, we used the spectrometer to determine the sugar content in Crown Pear. We purchased 64 samples from a local market in Changchun, China, and stored them at room temperature (25°C) for 24 h. From these, 40 samples were selected randomly to establish the calibration models, and 24 samples were used for as a prediction set. The instrument was warmed up for half an hour before the measurement. At the beginning of the experiment, the reference spectrum was obtained by measuring a white Teflon tile. As shown in

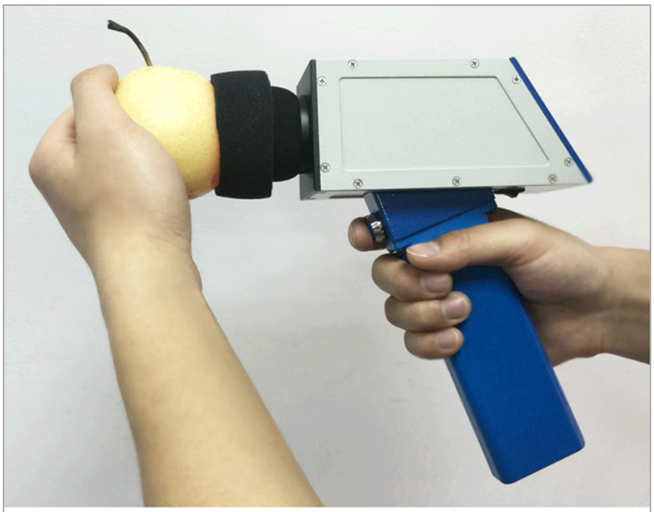

Figure 9. Spectra acquisition using the prototype spectrometer in interactance mode.

Table 1. Sugar content of pear samples.

Items	Max	Min	Mean	*SD*
Values (°Bx)	14.95	8.70	11.55	1.50

Figure 9, the spectrum of each pear was recorded in the equatorial region of the sample.

Brix measurements were recorded with a handheld refractometer (Model: LH-T20, Lohand Biological Co., Ltd, Hangzhou, China). Juice was extracted from the position where spectra were acquired. Table 1 summarises the Brix values.

Results and discussion

Key performance attributes

The instrument is compact and weighs less than 1 kg. The total power consumption of the electronics was only about 0.25 W, owing to the low power consumption of the detector, analogue-to-digital converter and other components. The total power consumption of the spectrometer was about 3 W, including the light source. Thus, the battery life was longer than 6 h. We used three laser modules to evaluate the spectral resolution of the instrument. As shown in Figure 10, the resolution (measured FWHM) was 9 nm at 650 nm, 11 nm at 785 nm and 14 nm at 980 nm. Each peak had an FWHM of less than 1.5% centre wavelength.

To assess the stability of the spectrometer, spectra for a white Teflon tile were measured with wireless control from a computer. The computer was programmed to trigger a measurement every minute over a period of 8 h. As 10 spectra were taken in a row during each measurement period, the computer displayed the standard deviation value of these 10 spectral intensities at each wavelength immediately. The standard deviation value was stable and was around 10 during the whole process, producing a signal-to-noise ratio of 5000. The spectral intensity stopped decreasing and remained stable after the lamp had been warmed up for approximately 30 min. In addition, we collected 20 spectra at 10-min intervals when the light source was stable, and calculated the standard deviation value. The value was around 10, the same as that for the above results. This indicated that the instrument was stable at room temperature.

Analytical performance

The computed absorbance spectra of 64 pear samples are shown in Figure 11. Models were developed using partial leas squares (PLS) regression with the full band of the absorbance spectra. Models were optimised by applying MSC, SNV and first derivative. Models using absorbance data without

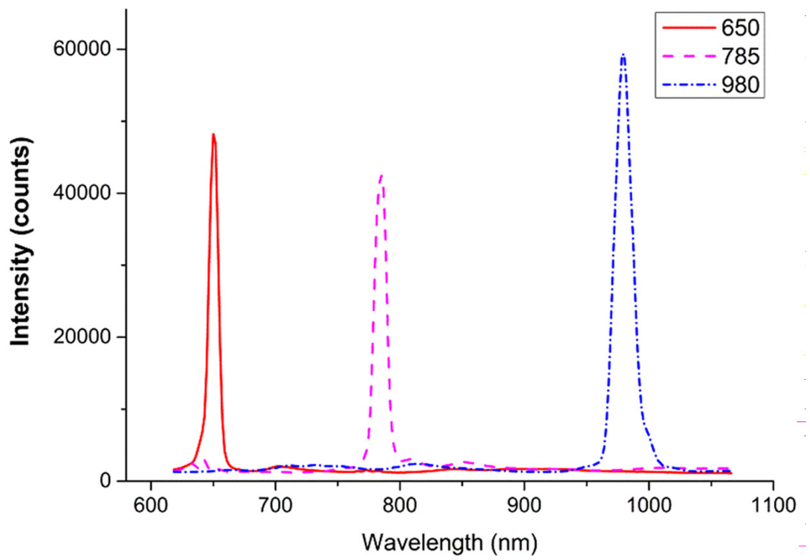

Figure 10. Measured results using a 650 nm, 785 nm and 980 nm laser.

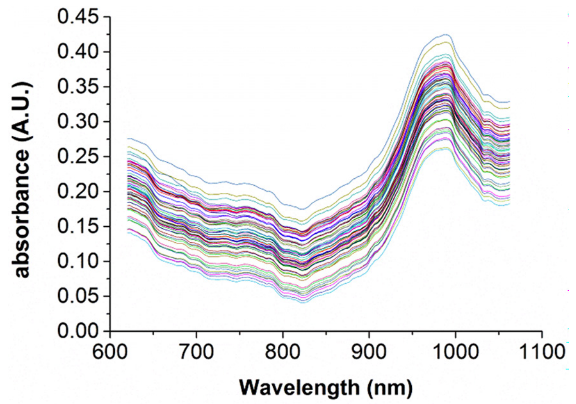

Figure 11. Computed absorbance spectra of all 64 pear samples in the 620~1060 nm region.

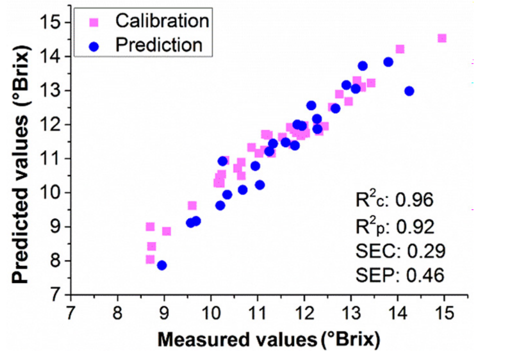

Figure 12. Scatter plots of predicted vs. measured °Brix for absorbance spectral data using the PLS method on the whole spectral range.

pretreatments showed the best precision (Figure 12). The coefficient of determination for calibration (R^2_c) was 0.96, the standard error of calibration (SEC) was 0.29 °Bx, and the standard error of prediction (SEP) was 0.46 °Bx. These results are comparable with those from other studies.[12]

Conclusion

A handheld spectrometer equipped with an LVF and a CMOS linear detector array has been designed to assess the internal quality of fruit. The LVF had a range of 620–1080 nm and was designed and fabricated specifically for this application. Using an LVF, a compact optical engine was obtained, providing a high degree of stability and ruggedness, low cost and a resolution of 1.5% centre wavelength. Using a CMOS detector, the spectrometer had a low power consumption and performed with a signal-to-noise ratio of up to 5000, which surpassed that of CCD-based handheld spectrometers.

The instrument can analyse spectral data using an onboard prediction model and can be operated wirelessly with a smartphone, tablet or laptop computer. An experiment carried out to predict sugar content in pears yielded optimised modelling results of R^2_c = 0.96, SEC = 0.29 °Bx and SEP = 0.46 °Bx. These results and the overall performance demonstrated that this LVF-based spectrometer is highly suitable for predicting fruit internal quality. However, modified software is needed, and further studies are required to test the performance of the spectrometer for predicting other attributes or detecting sugar in other fruits.

Acknowledgements

We are grateful for the continued financial support from the National High Technology Research and Development Program of China (2012AA022602), National Natural Science Foundation of China (61308067, 61475155), Jilin province Science and Technology Development Program item (20140204078GX) and the fund of State Key Laboratory of Applied Optics of China (Y2Q03FQZ01).

References

1. H. Lin and Y. Ying, "Theory and application of near infrared spectroscopy in assessment of fruit quality: a review", *Sens. Instrum. Food Qual. Saf.* **3,** 130 (2009). doi: http://dx.doi.org/10.1007/s11694-009-9079-z
2. K.B. Walsh, J.A. Guthrie and J.W. Burney, "Application of commercially available, low-cost, miniaturised NIR spectrometers to the assessment of the sugar content of intact fruit", *Funct. Plant Biol.* **27,** 1175 (2000). doi: http://dx.doi.org/10.1071/PP99111
3. J. Lammertyn, A. Peirs, J. De Baerdemaeker and B. Nicolaı, "Light penetration properties of NIR radiation in fruit with respect to non-destructive quality assessment", *Postharv. Biol. Technol.* **18,** 121 (2000). doi: http://dx.doi.org/10.1016/S0925-5214(99)00071-X
4. M. Alcalà, M. Blanco, D. Moyano, N. Broad, N. O'Brien, D. Friedrich, F. Pfeifer and H. Siesler, "Qualitative and quantitative pharmaceutical analysis with a novel handheld miniature near-infrared spectrometer", *J. Near Infrared Spectrosc.* **21,** 445 (2013). doi: http://dx.doi.org/10.1255/jnirs.1084
5. C. Biller, C. Hurburgh, N. Cao and G. Rippke, "Calibration of the JDSU MicroNir 1700 for agricultural product analysis", *NIR News* **25(6),** 16 (2014). doi: http://dx.doi.org/10.1255/nirn.1471
6. C.V. Greensill, P.J. Wolfs, C.H. Spiegelman and K.B. Walsh, "Calibration transfer between PDA-based NIR spectrometers in the NIR assessment of melon soluble solids content", *Appl. Spectrosc.* **55,** 647 (2001). doi: http://dx.doi.org/10.1366/0003702011952280
7. C.V. Greensill and K.B. Walsh, "Optimization of instrumentation precision and wavelength resolution for the performance of NIR calibrations of sucrose in a water-cellulose matrix", *Appl. Spectrosc.* **54,** 426 (2000). doi: http://dx.doi.org/10.1366/0003702001949528

8. B.M. Nicolaï, K. Beullens, E. Bobelyn, A. Peirs, W. Saeys, K.I. Theron and J. Lammertyn, "Nondestructive measurement of fruit and vegetable quality by means of NIR spectroscopy: a review", *Postharv. Biol. Technol*. **46,** 99 (2007). doi: http://dx.doi.org/10.1016/j.postharvbio.2007.06.024
9. P.N. Schaare and D.G. Fraser, "Comparison of reflectance, interactance and transmission modes of visible–near infrared spectroscopy for measuring internal properties of kiwifruit (*Actinidia chinensis*)", *Postharv. Biol. Technol*. **20,** 175 (2000). doi: http://dx.doi.org/10.1016/S0925-5214(00)00130-7
10. A. Piegari, I. Di Sarcina, M. Luisa Grilli, S. Scaglione and A. Sytchkova, "Optical transmission filters for observation of lightning phenomena in the Earth atmosphere", *Appl. Optics* **50,** C100 (2011). doi: http://dx.doi.org/10.1364/AO.50.00C100
11. M.T. Postek, B.R. Wiesent, D.G. Dorigo and A.W. Koch, "Limits of IR-spectrometers based on linear variable filters and detector arrays", in *Proceedings of SPIE 7767, Instrumentation, Metrology, and Standards for Nanomanufacturing IV*, 77670L (August 24, 2010). doi: http://dx.doi.org/10.1117/12.860532
12. J. Li, W. Huang, C. Zhao and B. Zhang, "A comparative study for the quantitative determination of soluble solids content, pH and firmness of pears by Vis/NIR spectroscopy", *J. Food Eng*. **116,** 324 (2013). doi: http://dx.doi.org/10.1016/j.jfoodeng.2012.11.007